THE JOURNAL OF PHYSICAL CHEMISTRY C
A JOURNAL OF THE AMERICAN CHEMICAL SOCIETY

pubs.acs.org/JPCC

Article

Periodic Precipitation of Zeolitic Imidazolate Frameworks in a Gelled Medium

Szabolcs Farkas, Máté Sándor Fonyi, Gábor Holló, Norbert Német, Nadia Valletti, Ákos Kukovecz, Gábor Schuszter, Federico Rossi, and István Lagzi*

Cite This: J. Phys. Chem. C 2022, 126, 9580−9586

Read Online

ACCESS | Metrics & More | Article Recommendations | Supporting Information

ABSTRACT: Formation of spatially periodic patterns is a ubiquitous process in nature and man-made systems. Periodic precipitation is the oldest type of pattern formation, in which the formed colloid particles are self-assembled into a sequence of spatially separated precipitation zones in solid hydrogels. Chemical systems exhibiting periodic precipitation mostly comprise oppositely charged inorganic ions. Here, we present a new sub-group of this phenomenon driven by the diffusion and reaction of several transition metal cations (Zn^{2+}, Co^{2+}, Cd^{2+}, Cu^{2+}, Fe^{2+}, Mn^{2+}, and Ni^{2+}) with an organic linker (2-methylimidazole) producing periodic precipitation of zeolitic imidazolate frameworks. In some cases, the formed crystals reached the size of ∼50 μm showing that a gel matrix can provide optimal conditions for nucleation and crystal growth. We investigated the effect of the gel concentration and solvent composition on the morphology of the pattern. To support the experimental observations, we developed a reaction−diffusion model, which qualitatively describes the spatially periodic pattern formation.

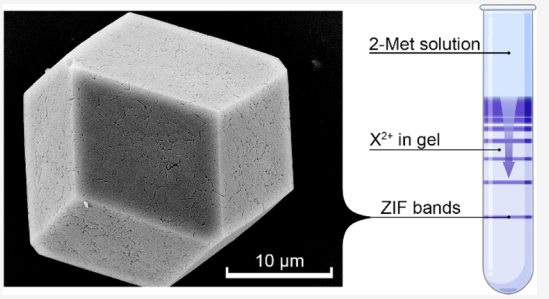

INTRODUCTION

Periodic precipitation (also known as the Liesegang phenomenon) is one of the oldest pattern formation phenomena executed in the laboratory.[1−4] The formed pattern structure consists of a spatially periodic appearance of the precipitate, which can be manifested in the formation of parallel bands (test tube) or concentric rings (radial spreading in thin gel layers) depending on the experimental setup. In these chemical systems, the coupling of the precipitation reaction to the diffusion of the reagents creates a pattern with the continuously increasing wavelength ranging between a few tens of micrometers to a few centimeters.[5,6] Recently, it has been presented that these systems offer a new route in material science to engineer and design layered hierarchical materials.[7−11] In a classical setup, the solutions of two water-soluble salts are spatially separated. One salt (called the inner electrolyte) is homogeneously dispersed in a hydrogel matrix (e.g., gelatin, agarose, polyacrylamide), and the other one diffuses in the gel (called the outer electrolyte). The concentration of the outer electrolyte is one or two orders of magnitude greater than that of the inner one. This difference in the concentrations of reagents ensures that the pattern formation is driven by the diffusion front of the invading electrolyte. The phenomenon has several hallmarks such as the distance between two consecutive bands and the width of the precipitation zones increasing with the band number.[12,13] The last 120 years of research on periodic precipitation have been focused on the chemical systems comprising hydrated (usually inorganic) ions.[2] In the past decade, the research of these reaction−diffusion systems shifted toward the pattern design using other types of building blocks such as charged nanoparticles[14,15] and gas-phase compounds in aerogels.[16,17] Recently, it has been demonstrated that the components of the zeolitic imidazolate framework-8 (ZIF-8), zinc ions and 2-methylimidazole (2-Met) molecules, in a gelled medium generated spatially continuous and periodic spatial appearance of ZIF-8 crystals with increasing size.[18,19] ZIFs are a special class of metal−organic frameworks (MOFs) that are topologically isomorphic with zeolites.[20−22] These materials have unique physical (e.g., great surface area and thermal stability) and chemical (e.g., significant transition metal containment) properties, and they are widely used in gas storage and separation, chromatography, electronics, organic chemical catalysts, and targeted drug delivery.[23−29] Therefore, the development of any novel synthesis methods plays a central role in the research of MOFs.

In our study, we extend the scope of the periodic precipitation to show that this phenomenon is not only limited to the reaction of inorganic ions, the interaction of

Received: April 7, 2022
Revised: May 9, 2022
Published: May 24, 2022

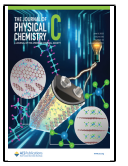

nanoparticles, and ZIF-8 precursors in the gel matrix but similar periodic structures can be obtained by the reaction and diffusion of various metal cations and an organic linker (2-Met). To support our experimental observations, a detailed reaction−diffusion model was developed consisting of the steps of the formation of ZIF-8 analogues.

EXPERIMENTAL SECTION

Gel Preparation. Agarose powder (Sigma-Aldrich, Type I) was dissolved in a mixture of distilled water and *N*,*N*-dimethylformamide (DMF, Sigma-Aldrich), and the mixture was continuously stirred using a magnetic stirrer (300 rpm) at 80−85 °C until complete dissolution of the agarose (∼10 min). Solution of cations ($ZnSO_4 \cdot H_2O$, $CoCl_2 \cdot 7H_2O$, $MgCl_2 \cdot 6H_2O$, $CdCl_2 \cdot 2.5H_2O$, $CuCl_2$, $FeCl_2 \cdot 4H_2O$, $MnCl_2 \cdot 4H_2O$, $NiCl_2 \cdot 6H_2O$, Sigma-Aldrich, dissolved in a mixture of distilled water and DMF) of various concentrations at room temperature (22 ± 0.5 °C) was added to the agarose solution. The homogenization was continued until the solutions reached 80−85 °C again, after which the solution was gently poured into test tubes (inner diameter and length of 8 mm and 10 cm, respectively) creating a gel column of 6 cm. The gelation process was accomplished in a refrigerator at ∼5 °C. After gelation (∼24 h), the gel column was allowed to rest for 1 h at room temperature and then a solution of 2-Met (Sigma-Aldrich, dissolved in a mixture of distilled water and DMF) was gently poured on top to create a liquid layer of 4 cm above the solid hydrogel column. All experiments were carried out at room temperature (22 ± 0.5 °C) usually for 1 week. In a set of experiments, all solutions contained the same ratio of DMF and distilled water.

In a reverse experimental setup, the 2-Met solution was added to the agarose solution and after gelation, a solution of $ZnSO_4$ was poured on top of the gel column. In addition, all experimental parameters were kept the same.

Samples Preparation for Scanning Electron Microscopy (SEM) and Powder X-ray Diffraction (PXRD) Measurements. The test tube containing the gel column was scratched with a glass cutting tool, and the tube was carefully broken. The gel was slid out and sliced up at the appropriate heights with a razor blade. The selected pieces of gel (∼0.3−0.5 mm) were put into Eppendorf tubes (2 mL) and dissolved in 1.5 mL DMF. The solution was centrifuged for 15 min at 7000 rpm, and the supernatant was carefully removed. The remaining precipitate was suspended in 1.5 mL DMF and centrifuged again. These cleaning steps were repeated three times. After the final centrifugation step, the samples were dried at ambient conditions.

SEM and PXRD Measurements. The formed crystals were investigated via SEM (Thermo scientific Apreo C) applying a secondary electron detector (Everhart−Thornley detector) and 10 kV accelerating voltage. The dry precipitate was placed onto a conducting tape, and gold sputtering was performed to maintain appropriate electrical conductance.

PXRD was applied to determine the crystalline phase of ZIF-67 crystals. The dry precipitate sample was placed on a monocrystalline silicon ingot and investigated with an X-ray diffractometer (Rigaku MiniFlex II Desktop X-ray Diffractometer) with Cu Kα (= 0.1542 nm) as a radiation source (30 kV accelerating voltage, 15 mA current) at ambient temperature in the 2Θ = 5−40 ° range applying a 0.02° step size.

RESULTS AND DISCUSSION

In a typical experiment, the metal cations (zinc(II), cobalt(II), cadmium(II), copper(II), iron(II), manganese(II), and nickel(II)) were homogeneously distributed in the agarose gel in test tubes. The aqueous environment does not create optimal conditions for the formation of ZIFs. The most frequently used solvent for the synthesis of ZIFs is DMF. Organic solvents facilitate the deprotonation of 2-Met and thus the coordination of the zinc ions with deprotonated 2-Met linkers. The generation of ZIF-8 in the aqueous phase significantly differs from the reaction steps in polar protic and aprotic solvents due to the different deprotonation mechanisms of 2-Met. The formation of ZIF-8 in an aqueous environment can be achieved only in a high excess of the linker. DMF was tested to create the solid gel structure using agarose in the 1:1 mixture with water. Greater DMF content did not generate a solid gel. Therefore, in most experiments, we used a 1:1 ratio of DMF and water for the preparation of the gel containing the inner electrolyte and the solution of the outer electrolyte as well. We did not adjust the pH in the experiments. After the gelation process (24 h), the solution of 2-Met was poured on top of the gel column. All experiments were carried out at room temperature (22 ± 0.5 °C). After 1 week, all test tubes were photographed and the formed ZIF-8 analogues were extracted from the gel matrix and subjected to scanning electron microscopy (SEM) measurements. The detailed experimental procedure and setup can be found in the Supporting Information (SI, Figure S1).

We started our investigation to reproduce the formation of periodic precipitation in the ZIF-8 (Zn^{2+}/2-Met) system (Figure S2)[19] and the generation of similar structures in the ZIF-67 (Co^{2+}/2-Met) system (Figure 1). In the literature,

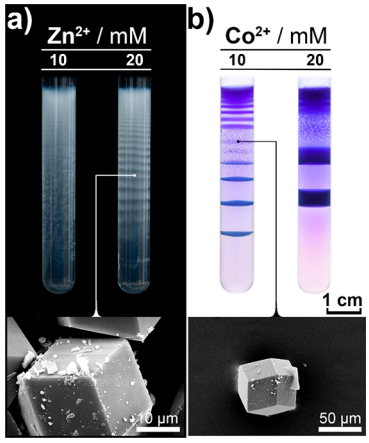

Figure 1. Periodic precipitation (optical photographs, upper part) and representative SEM micrographs (bottom part) of the formed crystals extracted from the gel matrix in ZIF-8 (a) and ZIF-67 (b) systems after 1 week of the reaction and diffusion of ZIF precursors at room temperature. The cations were homogeneously distributed in the agarose gel (0.5 m/V%, DMF/H_2O ratio was 1:1). The concentration of the outer electrolyte (2-Met) was 1.0 M.

periodic precipitation of ZIF-8 and mixed (Zn^{2+}/Co^{2+}) ZIF crystals has been previously reported.[19] However, no periodic precipitation (only formation of a continuous precipitation zone) was observed in the ZIF-67 system. In contrast to this observation, we report that a banded structure can be generated in both pure ZIF systems. One can notice that the

https://doi.org/10.1021/acs.jpcc.2c02371
J. Phys. Chem. C 2022, 126, 9580−9586

distance between the two consecutive bands in both systems is greater once the concentration of the cations increases (Figure 1). This is the manifestation of the Matalon–Packter law of the Liesegang system, namely, the spacing coefficient (defined as the ratio of distances of two consecutive bands measured from the gel–liquid interface) is linearly proportional to the concentration of the inner electrolyte (in this setup, the concentration of cations).[30−32]

We investigated the effect of the gel concentration on pattern formation because the usual argument in the periodic precipitation is that the gel does not contribute to the pattern formation. Its role is only to create a convection-free environment to prevent sedimentation of the formed precipitate. However, some recent studies pointed out that the gel can significantly affect the morphology of the pattern due to the change of the pore size and internal area of the gel.[33−35] Figure 2a shows the effect of the agarose

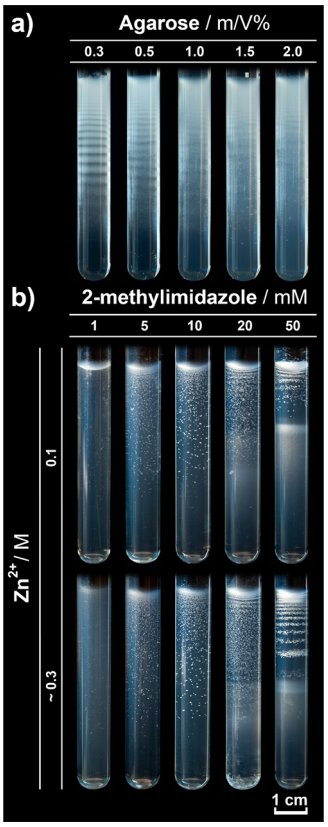

Figure 2. Periodic precipitation of the ZIF-8 system in the gel after 1 week of the reaction and diffusion of ZIF precursors at room temperature. (a) Effect of the gel concentration on the morphology of the pattern. The Zn^{2+} cation was homogeneously distributed in the agarose gel (0.5 m/V%, DMF/H_2O ratio was 1:1). The concentration of the outer electrolyte (2-Met) was 1.0 M. (b) ZIF-8 patterns in "revert" experiments, in which the 2-Met linker was homogeneously distributed in the agarose gel (0.5 m/V%, DMF/H_2O ratio was 1:1), while the zinc ions diffused from outside.

concentration on the patterns; increased gel concentration resulted in a continuous transition from the banded pattern to a continuous one. This transition can be explained by an increased agarose concentration that generates a denser gel matrix with an increased internal surface area facilitating heterogeneous nucleation events, which resulted in the continuous development of the precipitation zone.[35]

An important aspect of the synthesis of ZIFs in an aqueous phase is the usage of a significant excess of the organic linker with respect to the cations.[36−38] Usually, this concentration ratio varies between 10 and 50 and facilitates the formation of the charged cation–linker coordination complex, which is an intermediate in the generation of final sodalite polymorph (ZIF-8).[39] We carried out experiments in a "revert" experimental setup, namely, the zinc cations invaded from the outside having a higher concentration than that of the 2-Met in the gel (Figure 2b). Interestingly, in this case, we could observe periodic patterns consisting of small spheres (~0.1–0.3 mm) at a high concentration of 2-Met (50 mM). Once this concentration decreased, the periodicity of the pattern disappeared, but the formation of the macroscopic spherical precipitation particles sustained in the gel column produced a continuous distribution of these particles.

In the literature, it is well-known that other transition cations can coordinate to 2-Met generating various ZIF-8 analogues.[21,40] Other than zinc and cobalt cations, we selected five other cations: cadmium(II), copper(II), iron(II), manganese(II), and nickel(II). We obtained periodic precipitation of the ZIF-8 analogues in all cases (Figure 3). In cases

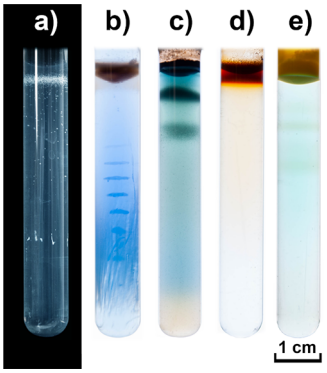

Figure 3. Precipitation structures of ZIF-8 analogues in the gel after 1 week of the reaction and diffusion of ZIF precursors at room temperature: (a) Cd^{2+}, (b) Cu^{2+}, (c) Fe^{2+}, (d) Mn^{2+}, and (e) Ni^{2+}. The cations were homogeneously distributed in the agarose gel (0.5 m/V%, DMF/H_2O ratio was 1:1) with the concentrations: $[Cd^{2+}]_0$ = 20 mM, $[Cu^{2+}]_0$ = 20 mM, $[Fe^{2+}]_0$ = 100 mM, $[Mn^{2+}]_0$ = 20 mM, $[Ni^{2+}]_0$ = 100 mM. The concentration of the outer electrolyte (2-Met) was 1.0 M.

of copper, iron, and nickel, the pattern consisted of several precipitation zones. However, in the case of cadmium and manganese, only one separate band formed near the gel–liquid interface. The whole range of the patterns formed at various inner electrolyte concentrations can be found in Figure S3.

In the synthesis of MOFs, the chemical composition of the solvent plays a crucial role in the final morphology, size, size distribution, and crystallinity of the particles. In the most widely used methods, the application of less polar solvents than water has been suggested due to the more effective deprotonation mechanism of 2-Met, which facilities the formation of ZIF crystals.[41] We carried out a series of experiments in ZIF-8 and ZIF-67 systems to investigate the effect of the solvent composition on the pattern structure. We used mixtures of DMF and water ranging from the volume ratio of 5:5 to 0:10 (DMF/water). At higher content of DMF, we could not perform experiments because the gelation was not completed producing a not solidified hydrogel matrix.

https://doi.org/10.1021/acs.jpcc.2c02371
J. Phys. Chem. C 2022, 126, 9580−9586

Figure 4 shows the obtained macroscopic patterns, and it can be seen that an increased DMF content in the solvent

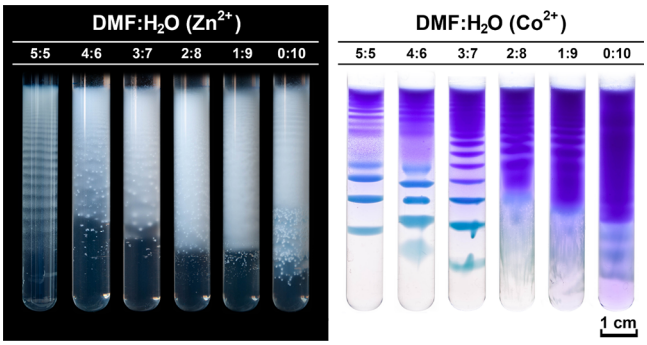

Figure 4. Effect of the solvent composition in ZIF-8 and ZIF-67 systems in the gel after 1 week of the reaction and diffusion of ZIF precursors at room temperature. The cations were homogeneously distributed in the agarose gel (0.5 m/V%). The concentration of the outer and inner electrolytes was $[Zn^{2+}]$ = 20 mM, $[Co^{2+}]$ = 10 mM and 1.0 M, respectively.

facilitated the formation of periodic precipitation in both systems. We found a transition from the periodic to continuous structure when the DMF content decreased (increasing the polarity of the solvent). This is because the deprotonation is higher in a less polar solvent and a big portion of 2-Met is present in a deprotonated form; therefore, the system behaves like the regular Liesegang system involving the reaction of oppositely charged ions. In contrast, a more polar environment hindered the deprotonation; the concentration of the deprotonated form of the linker decreased, and the excess of the outer electrolyte is not sufficient to generate periodic precipitation, similar to what happens in classic ionic systems when the concentration of the outer electrolyte is low.

To get more insight into the formation of ZIF-8 analogues, we characterized the formed crystals by using SEM. In Zn^{2+} and Co^{2+} systems, we found mostly octahedral-shaped crystals (Figure 1 and Figure S4a,b) indicating the formation of ZIF-8 and ZIF-67. To verify the formation of ZIF-67 crystals in the gel, we investigated the crystallinity of the crystals extracted from the gel matrix by using powder X-ray diffraction (PXRD, Figure S5). The XRD pattern shows excellent crystal structure (we did not perform PXRD of ZIF-8 crystals because it was already presented in the literature that ZIF-8 crystals formed in periodic precipitation in agarose gel have a crystalline structure and high porosity).[19] In revert experiments, in which the zinc ions (having greater concentration than that of 2-Met) invaded into a gel, the formation of plate-like crystals was observed (Figure S4c). Since in this setup, the high excess of the linker was not fulfilled, we hypothesize the formation of the thermodynamically most stable diamondoid topology framework.[42] In the case of cadmium ions, a few tens of micrometers of spherical particles were formed (Figure S4d). In other cases (copper, iron, manganese, and nickel cations), the precipitates consisted of submicrometer amorphous particles (Figure S4 e-h). It should be highlighted that using this diffusion-driven crystal growth method, we could generate ZIF-67 crystals with a size of ∼50 μm (Figure 1b), which is at least one order of magnitude greater compared to the crystal size obtained in bulk synthesis methods.[43−45]

To support our experimental findings, we developed a reaction−diffusion model incorporating the formation of ZIFs from the diffusion and reaction of cations and 2-Met. We developed the following kinetic model to describe the formation of ZIFs:

$$4L + M \rightarrow ML_4 \quad (1)$$

$$ML_4 + ML_4 \rightarrow 2ML_2 + 4L \quad (2)$$

$$ML_4 + ML_2 \rightarrow 2ML_2 + 2L \quad (3)$$

where L, M, ML_4, and ML_2 are the linker (2-Met), metal cation, coordination complex, and the final ZIF product, respectively. Equation 1 describes the coordination of the linker molecules to the cation forming a tetrahedral structure. The next step (eq 2) shows the formation of ZIF due to the aggregation of the complexes. Once the ZIF is formed, it can grow further by absorbing intermediates (eq 3). The reaction−diffusion system can be described mathematically in one dimension (along the gel column) by the following set of partial differential equations:

$$\frac{\partial l}{\partial t} = D_L \frac{\partial^2 l}{\partial x^2} - 4k_1 m l + 4k_2 c^2 \Theta(c - c^*) + 2k_3 c d \quad (4)$$

$$\frac{\partial m}{\partial t} = D_M \frac{\partial^2 m}{\partial x^2} - k_1 m l \quad (5)$$

$$\frac{\partial c}{\partial t} = D_C \frac{\partial^2 c}{\partial x^2} + k_1 m l - 2k_2 c^2 \Theta(c - c^*) - k_3 c d \quad (6)$$

$$\frac{\partial d}{\partial t} = 2k_2 c^2 \Theta(c - c^*) + k_3 c d \quad (7)$$

where l, m, c, and d are the concentrations of 2-Met, metal cation, metal−linker coordination complex (ML_4), and ML_2, respectively. It should be noted that the concentration of ML_2 represents the concentration of the building units of ZIFs in the system. In the model, the formation of the coordination complex is continuous. However, the generation of the ZIF structure from these complexes is a threshold limited step using the Heaviside step function, namely, the process occurs only if the concentration of the complex reaches a threshold concentration. This is a reflection of the existence of the solubility product. We solved the reaction−diffusion equations (eqs 4−7) numerically by using the method of lines technique on a 1D equidistant grid. The finite difference spatial discretization scheme was combined with a forward Euler method to solve the resulting set of ordinary differential equations. We applied the following initial conditions $l(t = 0, x) = 0.0$, $m(t = 0, x) = 2 \times 10^{-2}$, $c(t = 0, x) = 0$, and $d(t = 0, x) = 0$ to reflect the initial experimental conditions, namely, the metal cations were uniformly distributed in the gel matrix. We used Dirichlet and no-flux boundary conditions for all chemical species at $x = 0$ ($l(t,x = 0) = 1.0$, $m(t,x = 0) = c(t,x = 0) = d(t,x = 0) = 0$), and $x = N$ ($\left.\frac{\partial l}{\partial x}\right|_{x=N} = \left.\frac{\partial m}{\partial x}\right|_{x=N} = \left.\frac{\partial c}{\partial x}\right|_{x=N} = \left.\frac{\partial d}{\partial x}\right|_{x=N} = 0$), where N is the length of the simulation domain. The developed reaction−diffusion model could qualitatively reproduce the experimentally observed periodic banded structure (Figure 5a). The distance between two consecutive zones increased as the position of the band measured from the gel−liquid interface increased. Our model could reproduce the pattern transition induced by the gel concentration (Figure 5). The effect of the gel concentration was taken into account as the diffusion

https://doi.org/10.1021/acs.jpcc.2c02371
J. Phys. Chem. C 2022, 126, 9580−9586

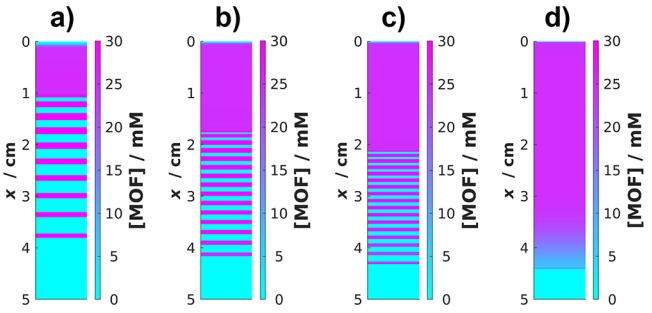

Figure 5. Spatial distribution of formed ZIFs in the gel matrix in the simulations varying the diffusion coefficient of the metal−linker coordination complex (a) $D_C = 5 \times 10^{-10}$ m^2 s^{-1}, (b) $D_C = 10^{-10}$ m^2 s^{-1}, (c) $D_C = 5 \times 10^{-11}$ m^2 s^{-1}, and (d) $D_C = 5 \times 10^{-12}$ m^2 s^{-1}. The following parameters were used: $D_L = D_M = 10^{-9}$ m^2 s^{-1}, $k_1 = 10^{-1}$ (Ms)$^{-1}$, $k_2 = 5 \times 10^{-4}$ (Ms)$^{-1}$, $k_3 = 5 \times 10^{-1}$ (Ms)$^{-1}$, $c^* = 5 \times 10^{-3}$ M. The grid spacing (Δx) and time step (Δt) in the numerical simulation were 5×10^{-4} m and 0.5 s, respectively.

coefficient of metal−linker coordination complex varies since denser gel (high gel concentration) has a smaller pore size and greater internal surface area inducing a decrease in the apparent diffusion coefficient of the complex.[35] The diffusion coefficients of the reagents, since those are small hydrated ions, were not changed in the simulations.

We performed a sensitivity study on how the reaction rate coefficients in the reaction−diffusion model affect the morphology of the pattern (Figure S6). We found that the most significant effect has k_3 (eq 3), and the less effective kinetic parameter is k_1 (eq 1). Varying k_3 from 5×10^{-2} to 5 (Ms)$^{-1}$, we could observe a crossover from a continuous pattern formation to a banded one (Figure S6c). During this process, the width of the zones decreased, but the number of the zones increased. Equation 3 represents the crystal growth; slow crystal growth (k_3 is small) favors the formation of continuous precipitation. However, when the crystal growth is fast (k_3 is high), the formed nuclei deplete the coordination complex in the vicinity of the nucleation site; thus, further nucleation (eq 2) can occur only farther from this nucleation site facilitating the formation of periodic precipitation (banded structure).

CONCLUSIONS

In conclusion, we have presented that periodic precipitation exists in various ZIF systems comprising transition metal cations and 2-Met. The main message of our results is that we can extend the universality of the periodic precipitation phenomenon known over 120 years. The Liesegang phenomenon is not limited to the precipitation of inorganic ions and nanoparticles, but a new sub-class of them is the system generated by diffusion and reactions of metal cations and organic linkers. We envisage other MOF systems in which similar pattern formation may occur. A big advantage of the synthesis of the MOFs in gelled media is that bigger and more tunable crystal size can be achieved than in classical bulk synthesis methods because the solid matrix ensures optimal conditions for the crystal growth through the reaction and diffusion of the reagents.[18,19]

ASSOCIATED CONTENT

Supporting Information

The Supporting Information is available free of charge at https://pubs.acs.org/doi/10.1021/acs.jpcc.2c02371.

Sketch of the experimental setup, periodic precipitation of ZIF-8 analogues, SEM micrographs of the formed particles, PXRD pattern of the ZIF-67 crystals formed in the gel, and results of the sensitivity study of the numerical model (PDF)

AUTHOR INFORMATION

Corresponding Author

István Lagzi − *Department of Physics, Institute of Physics and MTA-BME Condensed Matter Research Group, Budapest University of Technology and Economics, H-1111 Budapest, Hungary;* orcid.org/0000-0002-2303-5965; Phone: +361-463-1341; Email: lagzi.istvan.laszlo@ttk.bme.hu; Fax: +361-463-4180

Authors

Szabolcs Farkas − *Department of Physics, Institute of Physics, Budapest University of Technology and Economics, H-1111 Budapest, Hungary*

Máté Sándor Fonyi − *Department of Physics, Institute of Physics, Budapest University of Technology and Economics, H-1111 Budapest, Hungary*

Gábor Holló − *MTA-BME Condensed Matter Research Group, Budapest University of Technology and Economics, H-1111 Budapest, Hungary*

Norbert Német − *Department of Physics, Institute of Physics, Budapest University of Technology and Economics, H-1111 Budapest, Hungary*

Nadia Valletti − *Department of Earth, Environmental and Physical Sciences—DEEP Sciences, University of Siena, 53100 Siena, Italy*

Ákos Kukovecz − *Interdisciplinary Excellence Center, Department of Applied and Environmental Chemistry, University of Szeged, H-6720 Szeged, Hungary;* orcid.org/0000-0003-0716-9557

Gábor Schuszter − *Department of Physical Chemistry and Materials Science, University of Szeged, H-6720 Szeged, Hungary;* orcid.org/0000-0002-9170-9933

Federico Rossi − *Department of Earth, Environmental and Physical Sciences—DEEP Sciences, University of Siena, 53100 Siena, Italy;* orcid.org/0000-0002-1854-532X

Complete contact information is available at: https://pubs.acs.org/10.1021/acs.jpcc.2c02371

Author Contributions

The manuscript was written through contributions of all authors. All authors have given approval to the final version of the manuscript.

Notes

The authors declare no competing financial interest.

ACKNOWLEDGMENTS

This work was supported by the National Research, Development and Innovation Office of Hungary (K131425 and K138844) and the National Research, Development, and Innovation Fund of Hungary under Grant TKP2021-EGA-02.

REFERENCES

(1) Nakouzi, E.; Steinbock, O. Self-Organization in Precipitation Reactions Far from the Equilibrium. *Sci. Adv.* **2016**, *2*, No. e1601144.
(2) Nabika, H.; Itatani, M.; Lagzi, I. Pattern Formation in Precipitation Reactions: The Liesegang Phenomenon. *Langmuir* **2020**, *36*, 481−497.
(3) Müller, S. C.; Ross, J. Spatial Structure Formation in Precipitation Reactions. *J. Phys. Chem. A* **2003**, *107*, 7997−8008.
(4) Sadek, R.; Sultan, R. Liesegang Patterns in Nature: A Diverse Scenery Across the Sciences. In *Precipitation Patterns in Reaction-Diffusion Systems*; Research Signpost: Trivandrum, 2010; pp. 1−43.
(5) Smoukov, S. K.; Bitner, A.; Campbell, C. J.; Kandere-Grzybowska, K.; Grzybowski, B. A. Nano- and Microscopic Surface Wrinkles of Linearly Increasing Heights Prepared by Periodic Precipitation. *J. Am. Chem. Soc.* **2005**, *127*, 17803−17807.
(6) Klajn, R.; Fialkowski, M.; Bensemann, I. T.; Bitner, A.; Campbell, C. J.; Bishop, K.; Smoukov, S.; Grzybowski, B. A. Multicolour Micropatterning of Thin Films of Dry Gels. *Nat. Mater.* **2004**, *3*, 729−735.
(7) Badr, L.; Moussa, Z.; Hariri, A.; Sultan, R. Band, Target, and Onion Patterns in $Co(OH)_2$ Liesegang Systems. *Phys. Rev. E* **2011**, *83*, No. 016109.
(8) Ni, H.; Pan, M.; Shi, K.; Zhou, J.; Wu, M. Preparation of Isometric Liesegang Patterns and Application in Multi-Pulsed Drug Release System. *J. Sol-Gel Sci. Technol.* **2019**, *91*, 216−224.
(9) Ackroyd, A. J.; Holló, G.; Mundoor, H.; Zhang, H.; Gang, O.; Smalyukh, I. I.; Lagzi, I.; Kumacheva, E. Self-Organization of Nanoparticles and Molecules in Periodic Liesegang-Type Structures. *Sci. Adv.* **2021**, *7*, No. eabe3801.
(10) Ghaoui, J.; L'Heureux, I. Model of Layered Pattern Formation in Binary Igneous Systems. *Solid Earth Sci.* **2021**, *6*, 80−94.
(11) Konduktorova, A. A.; Kurochkina, V. A.; Babicheva, T. S.; Shmakov, S. L.; Shipovskaya, A. B. Study of the Supramolecularly Ordered Layered Structure of Chitosan Gel Films. *J. Phys.: Conf. Ser.* **2021**, *2086*, No. 012112.
(12) Droz, M.; Magnin, J.; Zrinyi, M. Liesegang Patterns: Studies on the Width Law. *J. Chem. Phys.* **1999**, *110*, 9618−9622.
(13) Walimbe, P. C.; Takale, K. D.; Kulkarni, P. S.; Kulkarni, S. D. Precise Evaluation of Spatial Characteristics of Periodically Precipitating Systems via Measurement of RGB (Red, Green, and Blue) Values of Pattern Images. *Langmuir* **2021**, *37*, 8212−8221.
(14) Lagzi, I.; Kowalczyk, B.; Grzybowski, B. A. Liesegang Rings Engineered from Charged Nanoparticles. *J. Am. Chem. Soc.* **2010**, *132*, 58−60.
(15) Itatani, M.; Fang, Q.; Lagzi, I.; Nabika, H. Phase Separation Mechanism for a Unified Understanding of Dissipative Pattern Formation in a Liesegang System. *Phys. Chem. Chem. Phys.* **2022**, *24*, 2088−2094.
(16) Samseth, J.; Kirkedelen, M. B.; Maaø, F. A.; Hansen, A.; Einarsrud, M.-A. Liesegang Pattern Formation by Gas Diffusion in Silica Aerogels. *J. Non-Cryst. Solids* **1998**, *225*, 298−302.
(17) Ramírez-Álvarez, E.; Montoya, F.; Buhse, T.; Rios-Herrera, W.; Torres-Guzmán, J.; Rivera, M.; Martínez-Mekler, G.; Müller, M. F. On the Dynamics of Liesegang-Type Pattern Formation in a Gaseous System. *Sci. Rep.* **2016**, *6*, 23402.
(18) Saliba, D.; Ammar, M.; Rammal, M.; Al-Ghoul, M.; Hmadeh, M. Crystal Growth of ZIF-8, ZIF-67, and Their Mixed-Metal Derivatives. *J. Am. Chem. Soc.* **2018**, *140*, 1812−1823.
(19) Zakhia Douaihy, R.; Al-Ghoul, M.; Hmadeh, M. Liesegang Banding for Controlled Size and Growth of Zeolitic-Imidazolate Frameworks. *Small* **2019**, *15*, 1901605.
(20) Tan, J. C.; Bennett, T. D.; Cheetham, A. K. Chemical Structure, Network Topology, and Porosity Effects on the Mechanical Properties of Zeolitic Imidazolate Frameworks. *Proc. Natl. Acad. Sci.* **2010**, *107*, 9938.
(21) Chen, B.; Yang, Z.; Zhu, Y.; Xia, Y. Zeolitic Imidazolate Framework Materials: Recent Progress in Synthesis and Applications. *J. Mater. Chem. A* **2014**, *2*, 16811−16831.
(22) Kouser, S.; Hezam, A.; Khadri, M. J. N.; Khanum, S. A. A Review on Zeolite Imidazole Frameworks: Synthesis, Properties, and Applications. *J. Porous Mater.* **2022**, 663.
(23) Song, Q.; Nataraj, S. K.; Roussenova, M. V.; Tan, J. C.; Hughes, D. J.; Li, W.; Bourgoin, P.; Alam, M. A.; Cheetham, A. K.; Al-Muhtaseb, S. A.; et al. Zeolitic Imidazolate Framework (ZIF-8) Based Polymer Nanocomposite Membranes for Gas Separation. *Energy Environ. Sci.* **2012**, *5*, 8359−8369.
(24) Han, S.; Wei, Y.; Valente, C.; Lagzi, I.; Gassensmith, J. J.; Coskun, A.; Stoddart, J. F.; Grzybowski, B. A. Chromatography in a Single Metal−Organic Framework (MOF) Crystal. *J. Am. Chem. Soc.* **2010**, *132*, 16358−16361.
(25) Aboraia, A. M.; Darwish, A. A. A.; Polyakov, V.; Erofeeva, E.; Butova, V.; Zahran, H. Y.; El-Rehim, A. F. A.; Algarni, H.; Yahia, I. S.; Soldatov, A. V. Structural Characterization and Optical Properties of Zeolitic Imidazolate Frameworks (ZIF-8) for Solid-State Electronics Applications. *Opt. Mater.* **2020**, *100*, 109648.
(26) Hu, H.; Liu, S.; Chen, C.; Wang, J.; Zou, Y.; Lin, L.; Yao, S. Two Novel Zeolitic Imidazolate Frameworks (ZIFs) as Sorbents for Solid-Phase Extraction (SPE) of Polycyclic Aromatic Hydrocarbons (PAHs) in Environmental Water Samples. *Analyst* **2014**, *139*, 5818−5826.
(27) Liu, Y.; Cheng, H.; Cheng, M.; Liu, Z.; Huang, D.; Zhang, G.; Shao, B.; Liang, Q.; Luo, S.; Wu, T.; et al. The Application of Zeolitic Imidazolate Frameworks (ZIFs) and Their Derivatives Based Materials for Photocatalytic Hydrogen Evolution and Pollutants Treatment. *Chem. Eng. J.* **2021**, *417*, 127914.
(28) Tran, U. P. N.; Le, K. K. A.; Phan, N. T. S. Expanding Applications of Metal−Organic Frameworks: Zeolite Imidazolate Framework ZIF-8 as an Efficient Heterogeneous Catalyst for the Knoevenagel Reaction. *ACS Catal.* **2011**, *1*, 120−127.
(29) Wang, Q.; Sun, Y.; Li, S.; Zhang, P.; Yao, Q. Synthesis and Modification of ZIF-8 and Its Application in Drug Delivery and Tumor Therapy. *RSC Adv.* **2020**, *10*, 37600−37620.
(30) Matalon, R.; Packter, A. The Liesegang Phenomenon. I. Sol Protection and Diffusion. *J. Colloid Sci.* **1955**, *10*, 46−62.
(31) Antal, T.; Droz, M.; Magnin, J.; Rácz, Z.; Zrinyi, M. Derivation of the Matalon-Packter Law for Liesegang Patterns. *J. Chem. Phys.* **1998**, *109*, 9479−9486.
(32) Itatani, M.; Fang, Q.; Nabika, H. Modification of the Matalon−Packter Law for Self-Organized Periodic Precipitation Patterns by Incorporating Time-Dependent Diffusion Flux. *J. Phys. Chem. B* **2021**, *125*, 6921−6929.
(33) Lagzi, I.; Ueyama, D. Pattern Transition between Periodic Liesegang Pattern and Crystal Growth Regime in Reaction−Diffusion Systems. *Chem. Phys. Lett.* **2009**, *468*, 188−192.
(34) Itatani, M.; Fang, Q.; Unoura, K.; Nabika, H. Programmable Design of Self-Organized Patterns through a Precipitation Reaction. *J. Phys. Chem. B* **2020**, *124*, 8402−8409.
(35) Rahbani, J.; Behzad, A. R.; Khashab, N. M.; Al-Ghoul, M. Characterization of Internal Structure of Hydrated Agar and Gelatin Matrices by Cryo-SEM. *Electrophoresis* **2013**, *34*, 405−408.
(36) He, M.; Yao, J.; Liu, Q.; Wang, K.; Chen, F.; Wang, H. Facile Synthesis of Zeolitic Imidazolate Framework-8 from a Concentrated Aqueous Solution. *Microporous Mesoporous Mater.* **2014**, *184*, 55−60.
(37) Choi, H.-S.; Lee, S.-J.; Bae, Y.-S.; Choung, S.-J.; Im, S. H.; Kim, J. Scalable Continuous Solvo-Jet Process for ZIF-8 Nanoparticles. *Chem. Eng. J.* **2015**, *266*, 56−63.
(38) Kolmykov, O.; Commenge, J.-M.; Alem, H.; Girot, E.; Mozet, K.; Medjahdi, G.; Schneider, R. Microfluidic Reactors for the Size-Controlled Synthesis of ZIF-8 Crystals in Aqueous Phase. *Mater. Des.* **2017**, *122*, 31−41.
(39) Jian, M.; Liu, B.; Liu, R.; Qu, J.; Wang, H.; Zhang, X. Water-Based Synthesis of Zeolitic Imidazolate Framework-8 with High Morphology Level at Room Temperature. *RSC Adv.* **2015**, *5*, 48433−48441.
(40) Pimentel, B. R.; Parulkar, A.; Zhou, E.; Brunelli, N. A.; Lively, R. P. Zeolitic Imidazolate Frameworks: Next-Generation Materials for

https://doi.org/10.1021/acs.jpcc.2c02371
J. Phys. Chem. C 2022, 126, 9580−9586

Energy-Efficient Gas Separations. *ChemSusChem* **2014**, *7*, 3202−3240.
(41) Akhundzadeh Tezerjani, A.; Halladj, R.; Askari, S. Different View of Solvent Effect on the Synthesis Methods of Zeolitic Imidazolate Framework-8 to Tuning the Crystal Structure and Properties. *RSC Adv.* **2021**, *11*, 19914−19923.
(42) Akimbekov, Z.; Katsenis, A. D.; Nagabhushana, G. P.; Ayoub, G.; Arhangelskis, M.; Morris, A. J.; Friščić, T.; Navrotsky, A. Experimental and Theoretical Evaluation of the Stability of True MOF Polymorphs Explains Their Mechanochemical Interconversions. *J. Am. Chem. Soc.* **2017**, *139*, 7952−7957.
(43) Qian, J.; Sun, F.; Qin, L. Hydrothermal Synthesis of Zeolitic Imidazolate Framework-67 (ZIF-67) Nanocrystals. *Mater. Lett.* **2012**, *82*, 220−223.
(44) Şahin, F.; Topuz, B.; Kalıpçılar, H. Synthesis of ZIF-7, ZIF-8, ZIF-67 and ZIF-L from Recycled Mother Liquors. *Microporous Mesoporous Mater.* **2018**, *261*, 259−267.
(45) Guo, Y.; Tang, J.; Qian, H.; Wang, Z.; Yamauchi, Y. One-Pot Synthesis of Zeolitic Imidazolate Framework 67-Derived Hollow Co_3S_4@MoS_2 Heterostructures as Efficient Bifunctional Catalysts. *Chem. Mater.* **2017**, *29*, 5566−5573.

https://doi.org/10.1021/acs.jpcc.2c02371
J. Phys. Chem. C 2022, 126, 9580−9586